Earth's Future

RESEARCH ARTICLE
10.1029/2021EF002019

Special Section:
CMIP6: Trends, Interactions, and Impacts.

Projected Changes to Hydroclimate Seasonality in the Continental United States

Kate Marvel[1,2], Benjamin I. Cook[1], Céline Bonfils[3], Jason E. Smerdon[4], A. Park Williams[4,5], and Haibo Liu[4]

[1]NASA Goddard Institute for Space Studies, New York, NY, USA, [2]Center for Climate Systems Research, Columbia University, New York, NY, USA, [3]Lawrence Livermore National Laboratory, Livermore, CA, USA, [4]Lamont-Doherty Earth Observatory, Palisades, NY, USA, [5]Now at Department of Geography, University of California, Los Angeles, Los Angeles, CA, USA

Abstract Future changes to the hydrological cycle are projected in a warming world, and any shifts in drought risk may prove extremely consequential for natural and human systems. In addition to long-term moistening, drying, or warming trends, perturbations to the annual cycle of regional hydroclimate variables may also have substantial impacts. We analyze projected changes in several hydroclimate variables across the continental United States, along with shifts in the amplitude and phase of their annual cycles. We find that even in regions where no robust change in the annual mean is expected, coherent changes to the annual cycle are projected. In particular, we identify robust regional phase shifts toward earlier arrival of peak evaporation in the northern regions, and peak runoff and total soil moisture in the western regions. Changes in the amplitude of the annual cycle of total and surface soil moisture are also projected, and reflect changes to the annual cycle in surface water supply and demand. Whether changes become detectable above the background noise of internal variability depends strongly on the future scenario considered, and significant changes to the annual cycle are largely avoided in the lowest-forcing scenario.

Plain Language Summary State-of-the-art climate models project substantial changes to the climate of the continental United States (CONUS). Models project changes to the yearly average rainfall, soil moisture, and runoff in many regions. But crucially, they also project changes to the annual cycle, with peaks in evaporation, runoff, and soil moisture projected to shift earlier in the year even if the yearly averages of those quantities do not change. While different climate models disagree on the exact nature of many shifts, a large source of uncertainty is human behavior and policy choices, and many significant changes can be avoided if greenhouse gas emissions fall drastically in the future.

Key Points:

- Coupled Model Intercomparison Project models project changes to the annual cycle of many hydroclimate variables, many of which are more significant than annual mean changes
- In the continental United States, there are significant earlier shifts in the annual cycle in a high emissions scenario
- Significant changes to the annual cycle are largely avoided in the lowest-emissions scenario

Supporting Information:

Supporting Information may be found in the online version of this article.

Correspondence to:

K. Marvel,
kate.marvel@nasa.gov

Citation:

Marvel, K., Cook, B. I., Bonfils, C., Smerdon, J. E., Williams, A. P., & Liu, H. (2021). Projected changes to hydroclimate seasonality in the continental United States. *Earth's Future*, *9*, e2021EF002019. https://doi.org/10.1029/2021EF002019

Received 2 FEB 2021
Accepted 16 JUL 2021

Author Contributions:

Conceptualization: Kate Marvel, Benjamin I. Cook, Céline Bonfils, Jason E. Smerdon
Formal analysis: Kate Marvel
Investigation: Kate Marvel, Benjamin I. Cook

1. Introduction

As the climate warms, the risk of disruption to human and natural systems increases. Changes to hydroclimate, particularly drought risk, have the potential to negatively affect lives, livelihoods, and ecosystems. Changes to major drivers of drought, including temperature (Bindoff et al., 2013), atmospheric water vapor (Santer et al., 2007), and precipitation (Marvel & Bonfils, 2013; Zhang et al., 2007) have already been detected and robustly attributed to human activity. Recent work has identified human influences on historical global drought trends (Marvel et al., 2019), on large-scale aridity trends (Bonfils et al., 2020) and the severity of individual regional droughts (Kelley et al., 2015; Williams et al., 2020). In the absence of major emissions reductions, these trends will continue to intensify; climate models project coherent changes to many aspects of the global hydrological cycle in the presence of elevated atmospheric CO_2 levels (Cook et al., 2020).

Despite the established work to date, there is still substantial uncertainty in projecting and understanding future hydroclimate changes (Hegerl et al., 2015; Sarojini et al., 2016), particularly at the smaller regional scales that are critical for adaptation decisions (Stott et al., 2010). There are several reasons for this. Even state-of-the-art general circulation models struggle to reproduce aspects of the observed hydrological cycle, especially precipitation (Levy et al., 2013; Marvel et al., 2013; Schneider et al., 2014; Tian & Dong, 2020). Climate models do not necessarily agree on the magnitude or sign of regional hydroclimate changes, and even robust regional trends may be difficult to identify against a backdrop of internal or naturally forced climate

Methodology: Kate Marvel, Benjamin I. Cook, Céline Bonfils, A. Park Williams
Software: Kate Marvel
Validation: Kate Marvel
Writing – original draft: Kate Marvel
Writing – review & editing: Kate Marvel, Benjamin I. Cook, Céline Bonfils, Jason E. Smerdon, A. Park Williams

variability (Bindoff et al., 2013; Cook et al., 2018; Stott et al., 2010). Projections of drought risk vary with the definition of drought used: changes to meteorological drought (a lack of rainfall) may differ from changes to agricultural (soil moisture) or hydrological (runoff) drought. Even within these categories, different variables are projected to respond differently to warming. For example, moisture may increase throughout the full soil column while drying at the surface (Berg et al., 2017), and evaporative demand from the warming atmosphere may be partially or fully offset by shifts in plant physiological response, resulting in quantitatively and qualitatively different responses depending on the variable considered (Bonfils et al., 2017; Mankin et al., 2019; Milly & Dunne, 2016; Swann et al., 2016).

Finally, in many regions, hydroclimate follows an annual cycle, with distinct wet and dry seasons. Even in areas where precipitation is relatively evenly distributed throughout the year, annual cycles in temperature, runoff, and evaporation can also shape annual cycles in soil moisture, both at the surface and throughout the soil column. Perturbations to this seasonality can have large societal impacts and compounding effects across multiple variables, even if there are no substantial changes to annual mean variables. It is therefore crucial for adaptation and planning purposes to quantify and understand shifts to both the amplitude and phase of the annual cycle.

Previous work has focused on understanding the mechanisms that underlie externally forced shifts in the amplitude of the annual cycle of different variables. Climate models project a weakened temperature annual cycle globally, due in large part to the disappearance of sea ice (Dwyer et al., 2012; Mann & Park, 1996; Santer et al., 2018). The amplitude of the annual cycle of precipitation, by contrast, is expected to increase on global scales (Chou & Lan, 2012; Dwyer et al., 2014; Marvel et al., 2017). In the absence of substantial changes to the atmospheric circulation, atmospheric water vapor increases by roughly 7 percent per degree Celsius of warming; global rainfall increases by only 2–3 percent per degree Celsius (Allen & Ingram, 2002; Pendergrass & Hartmann, 2014; Wentz et al., 2007) because of limits imposed by energetic constraints as well as moisture availability (O'Gorman & Schneider, 2009). On large scales, this creates a temporal "wet-get-wetter" effect, in which precipitation is expected to increase in wet seasons and decrease in dry seasons (Chou & Lan, 2012; Marvel et al., 2017). As with the spatial wet-get-wetter mechanism (Held & Soden, 2006), however, this simplification does not necessarily hold at regional scales, where local atmospheric dynamics, soil moisture holding capacity, and biogeochemical processes are important (Byrne & O'Gorman, 2015).

Models also project large-scale phase changes to many aspects of the hydrological cycle, including earlier snowmelt (Barnett et al., 2008) and spring phenology (Scranton & Amarasekare, 2017) and delayed rainfall onset in many monsoon regions (Neelin et al., 2003; Seth et al., 2013). Some of these trends and their consequences, such as earlier vegetation activity (Parmesan & Yohe, 2003) and elevated fire risk (Westerling, 2016), have been robustly detected in observations, but trends in many regions remain uncertain, reflecting complex seasonal interactions between multiple changing variables.

In this study, we examine future regional changes to the hydroclimate of the continental United States (CONUS). We report changes to both annual averages and annual cycles projected by the models participating in the most recent phase of the Coupled Model Intercomparison Project (CMIP6) and address three primary research questions: (a) What are the projected changes to meteorological, agricultural, and hydrological drought across different CONUS regions? (b) How will the annual cycle of hydroclimate in these regions change in the future? and (c) How does the emergence of a signal of forced change differ across different future forcing scenarios?

2. Methods

We investigate changes in eight monthly mean drought variables in the CMIP6 models: near-surface air temperature (CMIP6 variable name tas), evaporation (evspsbl), total precipitation (pr), the amount of precipitation that falls as snow (prsn), surface (mrros), and column-integrated total (mrro) runoff, and soil moisture at the surface (mrsos) and in the total column (mrso). Table 1 lists the 16 CMIP6 models and ensemble members that provided all eight of these diagnostics for the CMIP6 pre-industrial control experiment and each of four future forcing scenarios developed for ScenarioMIP (O'Neill et al., 2016). These

Table 1
The Number of Ensemble Members From Each Model's ScenarioMIP and Pre-Industrial Control Runs Used to Construct the Multi-Model CMIP6 Ensemble and Signal-to-Noise Ratios

	Reference	piControl	ssp126	ssp245	ssp370	ssp585
ACCESS-CM2	Dix et al. (2019)	1	1	1	1	1
ACCESS-ESM1-5	Ziehn et al. (2019)	1	3	3	3	3
BCC-CSM2-MR	Xin et al. (2019)	1	1	1	1	1
CESM2	Danabasoglu (2019)	1	2	3	2	2
CNRM-CM6-1	Voldoire (2019)	1	6	10	6	6
CNRM-ESM2-1	Seferian (2019)	1	5	5	5	5
CanESM5	Swart et al. (2019)	2	50	50	50	50
EC-Earth3	EC-Earth Consortium (EC-Earth) [2019a]	1	1	1	1	1
EC-Earth3-Veg	EC-Earth Consortium (EC-Earth) [2019b]	1	4	3	3	4
GFDL-ESM4	Guo et al. (2018)	1	1	3	1	1
IPSL-CM6A-LR	Boucher et al. (2018)	2	6	11	11	6
MIROC-ES2L	Tachiiri et al. (2019)	1	3	1	1	1
MIROC6	Shiogama et al. (2019)	1	3	3	3	3
MPI-ESM1-2-HR	Schupfner et al. (2019)	1	2	2	10	2
MRI-ESM2-0	Yukimoto et al. (2019)	2	1	5	5	2
UKESM1-0-LL	Good et al. (2019)	1	5	5	5	5

include the lowest-forcing scenario (SSP1-2.6), a medium forcing scenario (SSP2-4.5), and high-end forcing scenarios (SSP3-7.0 and SSP5-8.5).

The CMIP6 multi-model average (MMA) is calculated by first averaging over ensemble members of a single model, and then over results from all models. This ensures that the multi-model averages are not dominated by modeling groups that performed large ensembles. The models participating in CMIP6 do not necessarily span the entire space of plausible physical parametrizations (Eyring et al., 2016), nor do they constitute an independent ensemble. Rather than develop model weighting techniques that, while useful (Sanderson et al., 2017), necessarily rely on subjective criteria, we adopt a "one model, one vote" approach (Weigel et al., 2010), with the understanding that models may share code, parameterizations, and, in many cases entire modeling architectures (Masson & Knutti, 2011). Our amplitude and phase results are not highly sensitive to the order of operations; calculating and then averaging the amplitude and phase anomaly time series of individual ensemble members (Method A) leads to similar results as calculating the amplitude and phase changes of the multi-model average time series of monthly means (Method B). We use Method A in this study.

We calculate spatial averages over seven regions defined in Figure 1, designed to approximate the regions used in the Fourth National Climate Assessment (Reidmiller et al., 2017).

Each region is defined as a simple rectangle, which means there is some overlap between them. However, as these definitions vary and depend on cultural and political boundaries as well as aspects of the physical climate system, we elect for the simplicity of this approach for presenting summary statistics rather than attempt to replicate, for example, state boundaries. Monthly mean MMA changes in the highest-forcing SSP5-8.5 scenario for each region are shown in Figures S1–S7.

We track changes to the regional annual cycle in each variable, using a simple Fourier decomposition in each year (Stine et al., 2009). In each spatial region or model grid cell $\vec{x}$ and for each calendar year y, we calculate the mode with period 12 months:

$$F_{12}(\vec{x},y) = \frac{2}{12}\sum_{t=1/2}^{11/2} e^{2\pi i t/12} P(\vec{x},t+y) \quad (1)$$

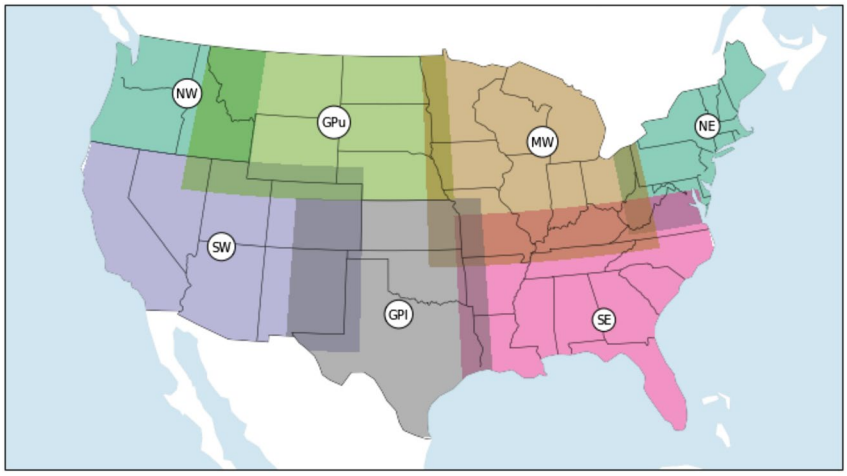

Figure 1. Geographical regions considered in this study: the Pacific Northwest (NW), southwest (SW), upper Great Plains (GPu), lower Great Plains (GPl), Midwest (MW), Northeast (NE), and Southeast (SE).

The amplitude is given by

$$R(\vec{x}, y) = \sqrt{\mathrm{Re}(F_{12}(\vec{x}, y))^2 + \mathrm{Im}(F_{12}(\vec{x}, y))^2} \tag{2}$$

and the phase by

$$\theta(\vec{x}, y) = \tan^{-1}\left\{\frac{\mathrm{Im}(F_{12}(\vec{x}, y))}{\mathrm{Re}(F_{12}(\vec{x}, y))}\right\} \times \frac{365}{2\pi}. \tag{3}$$

We calculate regional amplitude and phase changes by first performing the regional spatial average and then calculating the amplitude and phase of the resulting time series; spatially averaging the amplitude and phase for each grid cell in a region yields similar results.

To quantify the significance of projected changes against a backdrop of internal variability, we adopt a commonly used signal-to-noise framework (Santer et al., 1995, 2011, 2013). Here, the projected signal in each future scenario is defined to be the best-fit linear trend in the multi-model average annual mean, amplitude, or phase from 2015 to 2100. We compare these to the distribution of 86-year trends that would arise from internal variability alone. These are estimated from long time series obtained by concatenating the annual mean, amplitude, or phase of each CMIP6 model's pre-industrial control simulation, in which anthropogenic and natural forcings are fixed at their 1,850 values. The noise is defined as the standard deviation of the distribution of linear trends in all overlapping 86-year segments of these time series. The ratio of trends in the forced simulations to this noise term measures the forced trends' significance with respect to a null hypothesis that they arise purely due to internal variability. A projected signal is significant at the IPCC-defined "likely" threshold at 66% confidence, "very likely" at 90% confidence, and "virtually certain" at 99% confidence.

3. Results

3.1. Multi-Model Ensemble Average Trends

Figure 2 shows the projected 2015–2100 annual mean signal-to-noise ratios in each of the four scenarios.

In all regions, annual mean temperature robustly increases, with the warming signal detectable at high confidence in all scenarios (For visual clarity, we do not show these results because the signal-to-noise ratio is so large that its inclusion requires *y*-axis limits that obscure changes in other variables). Higher temperatures also reduce the total amount of precipitation falling as snow, but detectable changes to annual mean snow at the "very likely" level are avoided in the low-emissions scenario SSP1-2.6. However, despite reductions in snowfall, no region in the continental US is projected to experience a decrease in total precipitation. In fact,

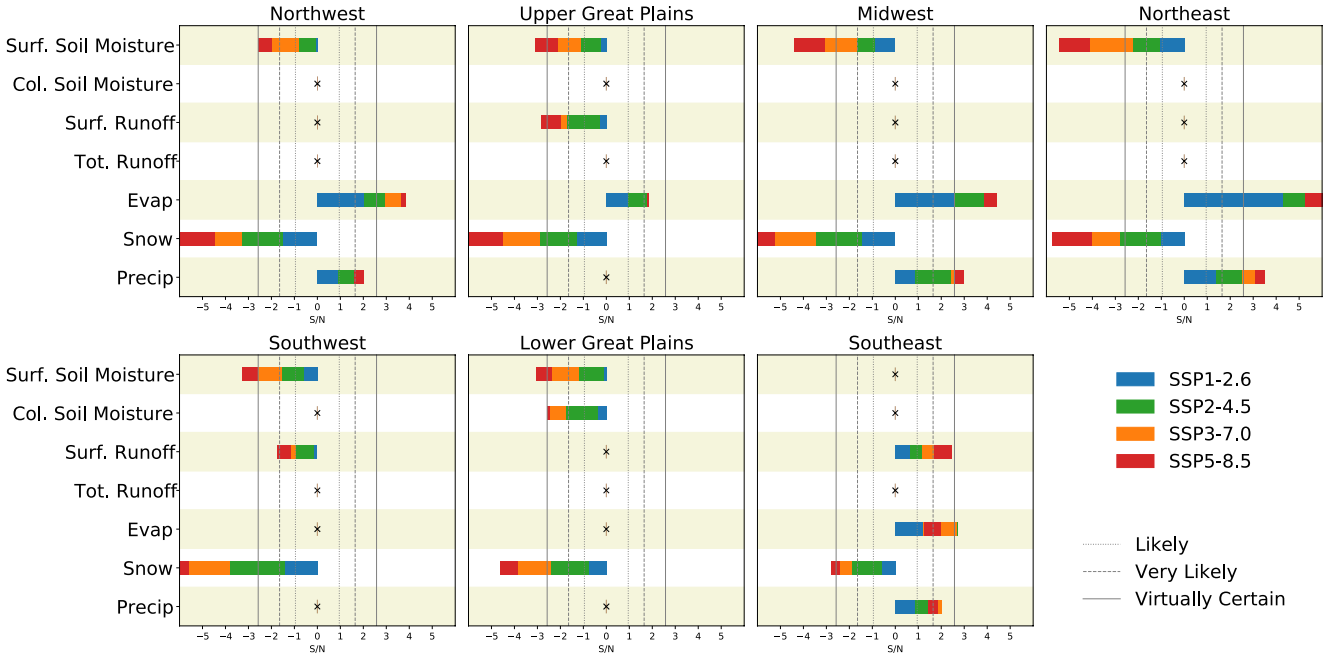

Figure 2. Signal-to-noise ratio for the annual mean of seven hydrological variables in four future scenarios spanning 2015–2100. Colors correspond to SSP1-2.6 (blue), SSP2-4.6 (green), SSP3-7.0 (orange), and SSP5-8.5 (red). We denote variables and regions where the signal-to-noise ratio never exceeds the IPCC "likely" standard (66% confidence) by a black cross.

under the highest emissions scenario, the models project a detectable increase in annual mean precipitation in four of the seven CONUS regions (the Northwest, Midwest, Northeast, and the Southeast). Annual mean evaporation increases are also apparent in these regions and in the upper Great Plains. Total and surface runoff changes are small in all regions except for the Southeast, where surface runoff is projected to increase. Only in the Lower Great Plains are there changes in annual mean total column-integrated soil moisture that exceed the "likely" threshold, and then only in the highest-forcing scenario. Total surface soil moisture decreases in every region, but the trend significance varies with region and forcing scenario.

Figure 3 shows projected changes to the amplitude of the annual cycle for each variable, scenario, and region. Every region is expected to experience decreased snowfall with warming and, because snow falls only in late fall through early spring, this translates to a decrease in the amplitude of the snow annual cycle. In the northern regions, models project an increase in the amplitude of the annual cycle of total column soil moisture that exceeds the "virtually certain" level in the two highest-forcing scenarios. In the Southwest, by contrast, the only detectable changes are to the amplitude of the annual cycle in surface soil moisture, which decreases. The amplitude of the annual cycle in precipitation increases in the Northwest and Southeast (although the climatological annual cycle in the latter region is both less regionally coherent and weaker in the latter region). The amplitude of the surface runoff annual cycle decreases in the Northwest, Southwest, and Great Plains, and increases in the Southeast; the amplitude of the total runoff annual cycle increases in the Midwest and Northeast.

Figure 4 shows projected changes to the phase of the annual cycle for each variable, scenario, and region. The only detectable changes are all in the negative direction: that is, in the future, the peak of many aspects of the water cycle is projected to arrive earlier. Evaporation phase shifts are detectable only in the northern regions, reflecting the roles of decreased snow cover, the increased evaporative demand that accompanies warming, and possibly an earlier start to the growing season. Shifts toward earlier peak rainfall are largest in the upper Great Plains and Midwest, and there are large differences between the SSP1-2.6 (in which changes are not significant) and SSP2-4.5 scenarios. Earlier snowpack melting combined with increases in wintertime precipitation, more of which falls as rain, mean that peak runoff in western regions is projected to shift earlier. Phase shifts in soil moisture in the northern and southwestern regions, most significantly in total soil moisture, only cross the "virtually certain" threshold in the highest-forcing scenario.

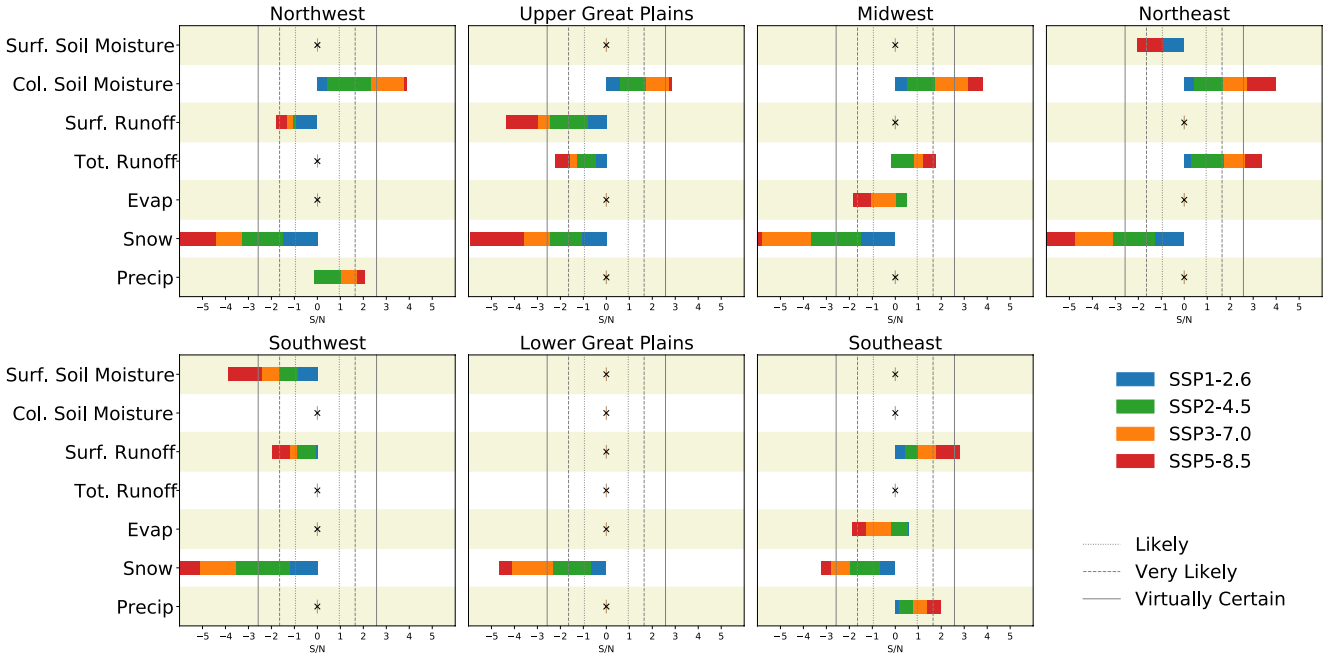

Figure 3. As in Figure 2, but for the amplitude of the annual cycle.

3.2. Robust Regional Trends in CMIP6

The results reported above are obtained from the average over multiple CMIP6 models. However, given the diverse treatments of the land surface (Hurk et al., 2016), a wider range of climate sensitivities (Meehl et al., 2020; Zelinka et al., 2020), and new parametrizations adopted by the CMIP6 climate models (Eyring et al., 2016), substantial inter-model differences might be expected. Moreover, climate models display biases: historically, they have struggled to reproduce precipitation (Scheff & Frierson, 2012; Tian & Dong, 2020), evapotranspiration (Mueller & Seneviratne, 2014), and runoff (Lehner et al., 2019) patterns at multiple

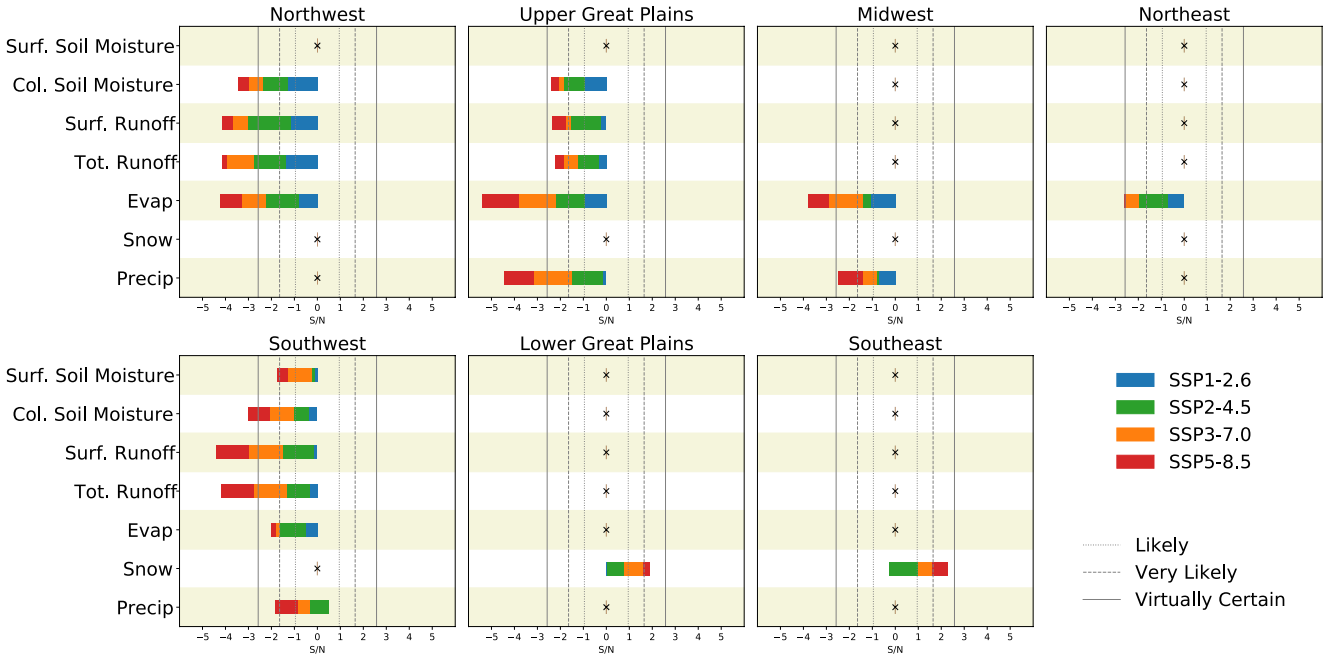

Figure 4. As in Figure 2, but for the phase of the annual cycle.

spatial (Marvel et al., 2013) and temporal (Sillmann et al., 2013) scales. However, despite model errors, CMIP6 models largely agree on many aspects of projected change, especially the most significant trends.

Figure 5 shows the CMIP6 model ensemble average regional SSP5-8.5 trends in the annual mean (blue), amplitude (orange) and phase (green) of the annual cycle. In order to plot variables of different units on the same scale, each model trend has been normalized by the same noise term obtained from the long concatenated pre-industrial control simulations. There are many areas where models agree on the trends in annual mean variables: robust declines in snow are projected everywhere, and precipitation changes are robustly positive in the Northeast and Midwest. Inter-model spread in total soil moisture trends is relatively small, despite the vastly different column depths used in CMIP6 models. However, substantial model disagreement persists, particularly in rainfall in the western regions and in the magnitude and even the sign of the total evaporation. Trends in regional annual cycles, however, are much more coherent across models. For example, while there is substantial model spread in annual mean precipitation trends in the upper Great Plains, the negative phase shift is robust across models. As a result, the amplitude of the total soil moisture annual cycle also robustly increases in models. Despite a large model spread in annual mean evaporation projections, most models project earlier peaks in evaporation across the northern regions.

CMIP6 models show a remarkable degree of coherence in the most significant hydroclimate projections. We define a significant effect to be a change to the annual mean, amplitude, or phase of the annual cycle that, in the multi-model average, exceeds the background of internal climate variability at the "virtually certain" level by 2100 in at least one future scenario. These regional effects are summarized in Tables 2–8, along with the fraction of the 16 CMIP6 models analyzed in which the signal is virtually certain to be detectable in 2100 in at least one scenario (F_{sig}) and the fraction of models in which the trend is of the same sign (F_{agree}). In some cases, individual CMIP6 models project large changes that are significant at high confidence levels but are of opposite sign to the multi-model average trends; the fraction of models in which this is the case is reported as F_{opp}.

3.2.1. Northwest

In the Northwest, as in most other regions, every CMIP6 model projects reductions in the annual mean snowfall, as well as in the amplitude of the snow annual cycle. Phase shifts in the column soil moisture, surface and total runoff, and evaporation are similarly robust, with over 80% of the models agreeing at least on the sign of the shift. Models disagree most on the annual mean evaporation, which increases in the multi-model average but is projected to decrease in three models (EC-Earth3, EC-Earth3-Veg, and MRI-ESM2-0).

3.2.2. Southwest

CMIP6 models largely agree on the most significant projections for the Southwest region (Table 3). Over half the models project significant decreases in surface soil moisture and its annual cycle, and earlier peaks in surface and total runoff are also robust across models. No CMIP6 model projects a detectable change of the opposite sign to the multi-model average.

3.2.3. Upper Great Plains

The degree to which models agree is perhaps even more pronounced in the upper Great Plains region (Table 4). Here, 100% of CMIP6 models analyzed here project an earlier peak in precipitation, with the change detectable above internal variability at the "virtually certain" level in all but one model (in which it is detectable at the "very likely" level). There is virtually no disagreement among CMIP6 models that peak evaporation in this region will arrive earlier, that the amplitude of total soil moisture and surface runoff will decrease, and that the region will experience surface soil moisture drying, although models disagree on the severity of the latter effect.

3.2.4. Lower Great Plains

Fewer significant changes are projected for the lower Great Plains region (Table 5). Models largely agree that surface and total soil moisture will dry in the future, but disagree on how significant these changes will be with respect to internal climate variability.

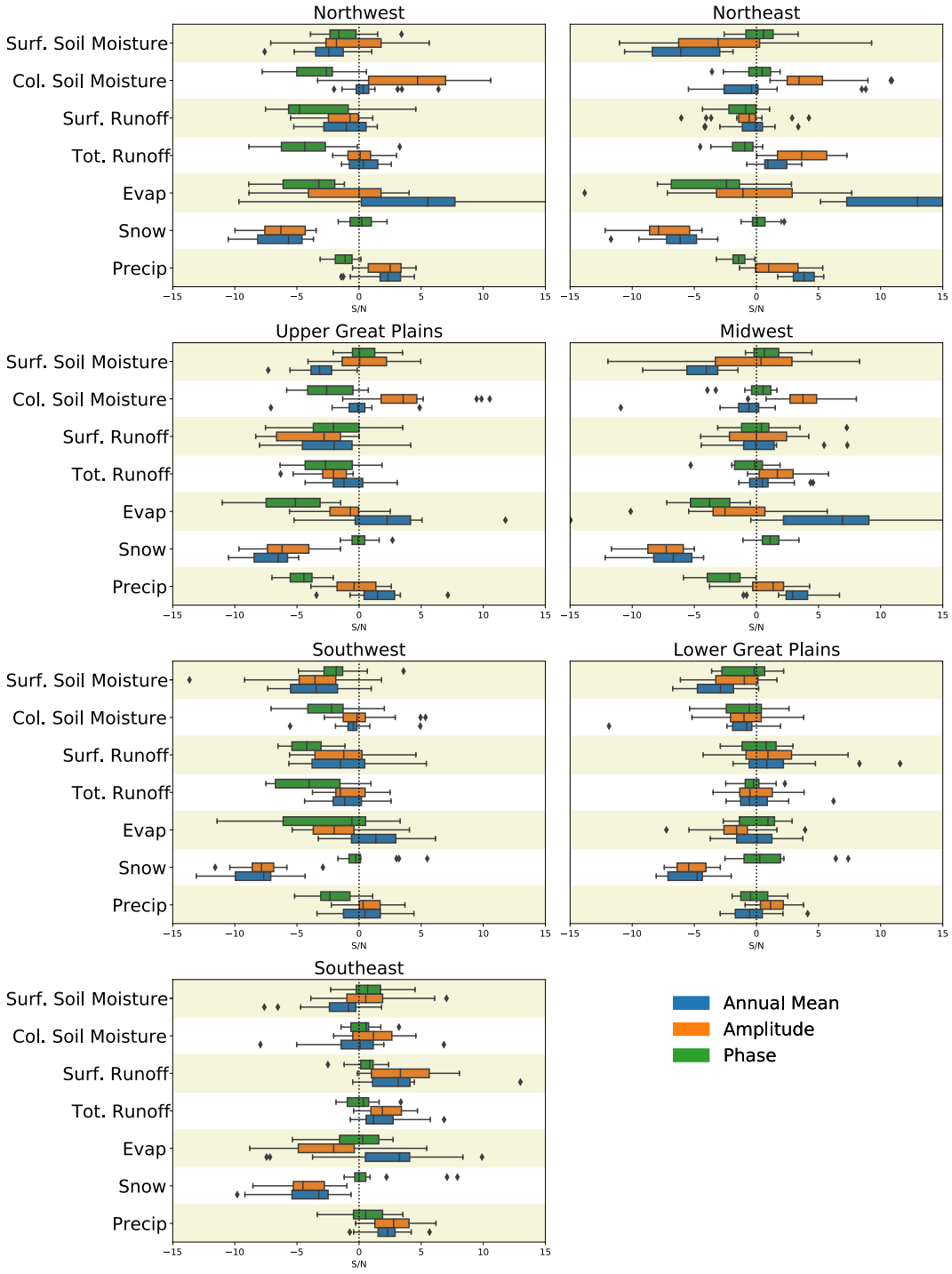

Figure 5. Box-and-whisker plots showing CMIP6 inter-model spread in SSP5-8.5 trends in the annual mean (blue), amplitude (orange) and phase (green) of the annual cycle. The boxes show the quartiles of the datasets while the whiskers represent the interquartile range multiplied by 1.5. Only the first ensemble member of each model is included in this calculation.

3.2.5. Midwest

In the Midwest, as in the adjacent upper Great Plains region, all CMIP6 models project that peak precipitation will shift earlier in the year (Table 6), and most models agree that the annual mean precipitation will

Table 2
Significant Effects Projected by CMIP6 Models for the Northwest, the Fraction $\mathbf{F}_{sig}$ of Models in Which the Signal is "Virtually Certain" to Emerge by 2100, the Fraction $\mathbf{F}_{agree}$ of Models in Which the Trend is of the Same Sign, and the Fraction $\mathbf{F}_{opp}$ of Models That Project Significant Changes of the Opposite Sign

Variable	Effect	$\mathbf{F}_{sig}$	$\mathbf{F}_{agree}$	$\mathbf{F}_{opp}$
Surface soil moisture	Annual mean decreases	0.5	0.9375	0.0
Column-integrated soil moisture	Annual cycle amplitude increases	0.6875	0.8125	0.0625
	Peak arrives earlier	0.5	0.9375	0.0
Surface runoff	Peak arrives earlier	0.6875	0.8125	0.0625
Total runoff	Peak arrives earlier	0.75	0.9375	0.0625
Evaporation	Annual mean increases	0.6875	0.75	0.1875
	Peak arrives earlier	0.6875	1.0	0.0
Precipitation falling as snow	Annual mean decreases	1.0	1.0	0.0
	Annual cycle amplitude decreases	1.0	1.0	0.0

increase. Despite this, all models project drying in the annual mean surface soil moisture. While most models project that the annual mean evaporation will increase, three outliers (as in the Northwest and, below, in the Northeast) project significant decreases. Models also agree on the sign, if not necessarily the magnitude, of changes to surface and column-integrated soil moisture.

3.2.6. Northeast

In the Northeast, all 16 models analyzed agree on the sign of all significant projected changes (Table 7) except for those to evaporation, which three models (as in the Midwest and Northwest, EC-Earth3, EC-Earth3-Veg, and MRI-ESM2-0) project will significantly decrease and one model (ACCESS-ESM1-5) projects will peak later.

3.2.7. Southeast

Finally, in the Southeast, models largely agree on the signs (earlier peaks in total and surface runoff, decreases in annual mean and the annual cycle amplitude of surface soil moisture) of projected trends (Table 8), although significant changes are not projected in every model.

4. Discussion

The results presented in the previous section indicate that (a) models agree on many robust regional changes to the hydroclimate of the continental United States and (b) significant changes to aspects of the annual cycle may arise even in the absence of changes to annual mean quantities. In this section, we show that understanding projected changes to the annual cycle can help to identify connections between variables

Table 3
Significant Effects Projected by CMIP6 Models for the Southwest, the Fraction $\mathbf{F}_{sig}$ of Models in Which the Signal is "Virtually Certain" to Emerge by 2100, the Fraction $\mathbf{F}_{agree}$ of Models in Which the Trend is of the Same Sign, and the Fraction $\mathbf{F}_{opp}$ of Models That Project Significant Changes of the Opposite Sign

Variable	Effect	$\mathbf{F}_{sig}$	$\mathbf{F}_{agree}$	$\mathbf{F}_{opp}$
Surface soil moisture	Annual mean decreases	0.625	0.8125	0.0
	Annual cycle amplitude decreases	0.625	0.9375	0.0
Surface runoff	Peak arrives earlier	0.75	1.0	0.0
Total runoff	Peak arrives earlier	0.6875	0.9375	0.0
Precipitation falling as snow	Annual mean decreases	1.0	1.0	0.0
	Annual cycle amplitude decreases	1.0	1.0	0.0

Table 4
Significant Effects Projected by CMIP6 Models for the Upper Great Plains, the Fraction $\mathbf{F}_{sig}$ of Models in Which the Signal is "Virtually Certain" to Emerge by 2100, the Fraction $\mathbf{F}_{agree}$ of Models in Which the Trend is of the Same Sign, and the Fraction $\mathbf{F}_{opp}$ of Models That Project Significant Changes of the Opposite Sign

Variable	Effect	$\mathbf{F}_{sig}$	$\mathbf{F}_{agree}$	$\mathbf{F}_{opp}$
Surface soil moisture	Annual mean decreases	0.5625	1.0	0.0
Column-integrated soil moisture	Annual cycle amplitude increases	0.6875	0.875	0.0
Surface runoff	Annual cycle amplitude decreases	0.5	0.875	0.0
Evaporation	Peak arrives earlier	0.8125	1.0	0.0
Precipitation falling as snow	Annual mean decreases	1.0	1.0	0.0
	Annual cycle amplitude decreases	0.9375	1.0	0.0
Precipitation	Peak arrives earlier	0.9375	1.0	0.0

and advance understanding of the underlying physical drivers of change. Hydrological and agricultural drought risks are shaped by changes in moisture supply and demand, but the timing of these changes and how they intersect with existing seasonal patterns may lead to different projections for runoff and soil moisture, and different management strategies.

4.1. Precipitation and Evaporation

Figure 6 shows projected changes to the timing and amount of precipitation and evaporation in the highest-forcing SSP5-8.5 scenario. In the multi-model average, precipitation is projected to increase outside the southernmost regions, and models largely agree on the sign of these changes in the eastern and western portions of the country. These wet trends are accompanied by increased evaporation in the same regions. Changes to the annual cycle amplitudes, however, reveal differences in the temporal structure of these changes. The amplitude of the precipitation annual cycle increases in the Northwest and Southeast, as more precipitation falls in the winter-wet season. The evaporation annual cycle, by contrast, decreases nearly everywhere in the multi-model average, and there is a high degree of inter-model agreement on this trend in the central regions. This indicates that evaporation increases are largest outside the peak summer season. In northern regions, there are shifts (Figure 6f) to earlier peak evaporation that may be associated with reductions in snow cover and warmer temperatures that in turn allows for photosynthesis and transpiration to begin earlier in the year (Mankin et al., 2017). In southern regions evaporation remains unchanged or even decreases in the summer: temperature-driven evaporative demand increases, there is no compensating increase in precipitation, runoff is negligible, and the soil becomes simply too dry to lose any more moisture. The patterns of projected phase shifts in moisture supply and demand are largely similar, with earlier peaks in precipitation projected in the northern and central regions. Notably, while no changes to total precipitation are projected in the Midwest and upper Great Plains, models robustly project an earlier shift of the precipitation annual cycle in these regions. Here, a large proportion of annual mean precipitation falls in spring and summer, with mesoscale convective systems contributing the bulk of warm-season rainfall (Schumacher & Rasmussen, 2020). The projected phase shift in this precipitation may be associated with

Table 5
Significant Effects Projected by CMIP6 Models for the Lower Great Plains, the Fraction $\mathbf{F}_{sig}$ of Models in Which the Signal is "Virtually Certain" to Emerge by 2100, the Fraction $\mathbf{F}_{agree}$ of Models in Which the Trend is of the Same Sign, and the Fraction $\mathbf{F}_{opp}$ of Models That Project Significant Changes of the Opposite Sign

Variable	Effect	$\mathbf{F}_{sig}$	$\mathbf{F}_{agree}$	$\mathbf{F}_{opp}$
Surface soil moisture	Annual mean decreases	0.625	0.875	0.0
Column-integrated soil moisture	Annual mean decreases	0.125	0.875	0.0
Precipitation falling as snow	Annual mean decreases	0.875	1.0	0.0
	Annual cycle amplitude decreases	1.0	1.0	0.0

Table 6
Significant Effects Projected by CMIP6 Models for the Midwest, the Fraction $\mathbf{F}_{sig}$ *of Models in Which the Signal is "Virtually Certain" to Emerge by 2100, the Fraction* $\mathbf{F}_{agree}$ *of Models in Which the Trend is of the Same Sign, and the Fraction* $\mathbf{F}_{opp}$ *of Models That Project Significant Changes of the Opposite Sign*

Variable	Effect	$\mathbf{F}_{sig}$	$\mathbf{F}_{agree}$	$\mathbf{F}_{opp}$
Surface soil moisture	Annual mean decreases	0.8125	1.0	0.0
Column-integrated soil moisture	Annual cycle amplitude increases	0.75	0.9375	0.0
Evaporation	Annual mean increases	0.75	0.8125	0.125
	Peak arrives earlier	0.6875	1.0	0.0
Precipitation falling as snow	Annual mean decreases	1.0	1.0	0.0
	Annual cycle amplitude decreases	1.0	1.0	0.0
Precipitation	Annual mean increases	0.6875	0.875	0.0
	Peak arrives earlier	0.375	1.0	0.0

warming temperatures that increase convective available potential energy (Diffenbaugh et al., 2013; Seeley & Romps, 2015) earlier in the year or an intensification of the low-level jet (Tang et al., 2017), but despite their different resolutions and climatologies, all CMIP6 models considered robustly project wintertime precipitation increases and decreases throughout the late spring and summer.

4.2. Runoff

These changes have implications for hydrological drought risk. Figure 7 shows projected changes to the timing and amount of surface and total runoff. Broadly, under SSP5-8.5, annual mean runoff decreases sharply in the northern and western regions and increases in the south and east. This spatial pattern is driven largely by the timing of projected changes in precipitation and the role of snow (Barnett et al., 2008). West of the Rockies, winter is the wettest season, and runoff has historically peaked in spring with the melting of the mountain snowpack (Lehner et al., 2019; Milly et al., 2005; Wood et al., 1997). A projected increase in wintertime precipitation does not translate into increases in springtime runoff, because far less of this precipitation falls as snow and the mountain snowpack consequently decreases. There is a robust decrease in the annual cycle amplitude and a phase shift toward an earlier peak of runoff (surface and total) due to the earlier disappearance of this snowpack. However, there is almost no role for mountain snowpack in the eastern regions. An increase in precipitation throughout the winter and early spring directly translates into increased runoff in the southeast, where snowfall is negligible. In the Northeast, total precipitation is projected to increase outside the summer months, and less of this precipitation is expected to fall as snow.

Table 7
Significant Effects Projected by CMIP6 Models for the Northeast, the Fraction $\mathbf{F}_{sig}$ *of Models in Which the Signal is "Virtually Certain" to Emerge by 2100, the Fraction* $\mathbf{F}_{agree}$ *of Models in Which the Trend is of the Same Sign, and the Fraction* $\mathbf{F}_{opp}$ *of Models That Project Significant Changes of the Opposite Sign*

Variable	Effect	$\mathbf{F}_{sig}$	$\mathbf{F}_{agree}$	$\mathbf{F}_{opp}$
Surface soil moisture	Annual mean decreases	0.8125	1.0	0.0
Column-integrated soil moisture	Annual cycle amplitude increases	0.625	1.0	0.0
Total runoff	Annual cycle amplitude increases	0.5625	1.0	0.0
Evaporation	Annual mean increases	0.875	0.875	0.125
	Peak arrives earlier	0.4375	0.875	0.0625
Precipitation falling as snow	Annual mean decreases	1.0	1.0	0.0
	Annual cycle amplitude decreases	1.0	1.0	0.0
Precipitation	Annual mean increases	0.9375	1.0	0.0

Table 8
Significant Effects Projected by CMIP6 Models for the Southeast, the Fraction $\mathbf{F}_{sig}$ of Models in Which the Signal is "Virtually Certain" to Emerge by 2100, the Fraction $\mathbf{F}_{agree}$ of Models in Which the Trend is of the Same Sign, and the Fraction $\mathbf{F}_{opp}$ of Models That Project Significant Changes of the Opposite Sign

Variable	Effect	$\mathbf{F}_{sig}$	$\mathbf{F}_{agree}$	$\mathbf{F}_{opp}$
Surface runoff	Annual mean increases	0.5625	0.875	0.0
	annual cycle amplitude increases	0.5625	0.9375	0.0
Precipitation falling as snow	Annual mean decreases	0.625	1.0	0.0
	annual cycle amplitude decreases	0.875	1.0	0.0
Precipitation	annual cycle amplitude increases	0.5625	0.875	0.0

This leads to an increase in total runoff, but a decrease in springtime surface runoff due to reduced snowfall and hence melt-driven runoff.

4.3. Soil Moisture

Precipitation, evaporation, and runoff changes also shape future agricultural drought risk. Figure 8 shows projected changes to the timing and amount of surface and column-integrated soil moisture. As in the previous generation of climate models (Cook et al., 2015), there are differences between trends at the surface and trends deeper in the soil column. Annual mean surface soil moisture dries everywhere in most CMIP6 models, although model disagreement is largest in the Southeast. Despite the small and uncertain annual mean trends in column-integrated soil moisture, there is a striking contrast between column soil moisture amplitude trends in the northern and southern parts of CONUS, particularly in the west. This difference is due to changes in the timing of moisture supply, as well as shifts in evaporative demand. In the Northwest, total column soil moisture robustly increases in the winter months and remains relatively unchanged otherwise (Figure S1). This is very likely a consequence of the projected increase in wintertime precipitation, which leads to an increase in the total soil moisture during the main precipitation season (November through March). Moreover, more of this precipitation is projected to fall as rain instead of snow (Hamlet et al., 2005; Knowles et al., 2006), actively recharging the soils when, historically, it would have been stored as snow and released in a large runoff event in spring (Barnett et al., 2005; Dettinger & Cayan, 1995). This extra moisture can carry through the deeper layers and compensate for low rainfall in the summer. The shallow surface layers, by contrast, are more responsive to warming than the full soil moisture column, and indeed are responding to large projected temperature increases in every season. Consequently, the *surface* soil moisture in the Northwest is projected by the CMIP6 multi-model average to decrease relatively uniformly throughout the year (Figure S1). The surface soil moisture is also responding to seasonal shifts in total surface evaporation, which shifts earlier in the year due to reductions in snow cover and warmer temperatures that in turn allows for photosynthesis and transpiration to begin earlier in the year (Mankin et al., 2017). In the Southwest, the total column soil moisture decreases throughout the year (Figure S2), with the largest declines in the late winter and early spring when soil moisture is at its maximum (and hence, a reduction in the amplitude of the annual cycle). Little change is projected in annual mean precipitation, with small increases in the winter and decreases in the spring, and therefore the region is not projected to benefit from the same seasonal increase in moisture supply seen in the Northwest (Cook et al., 2021). The region will similarly not see an appreciable phase shift in evaporation: having little snow cover to begin with, vegetation in the Southwest will not necessarily experience earlier photosynthesis due to reductions in snow. Moreover, evaporation is projected to decrease throughout the summer months when surface soil moisture is at its lowest. This indicates that in the season of peak evaporative demand, there will be no compensating increase in precipitation, and the supply drawn from the surface soil layers will be exhausted. In the Northeast (Figure S6) and Southeast (Figure S7), surface soil moisture decreases even as total runoff increases. An examination of the seasonality helps to explain this apparent paradox (Cook et al., 2020). In the Southeast, a small increase in precipitation in late winter and early spring, almost none of which is stored in snowpack, leads to an increase in moisture availability at the time when soil moisture is most

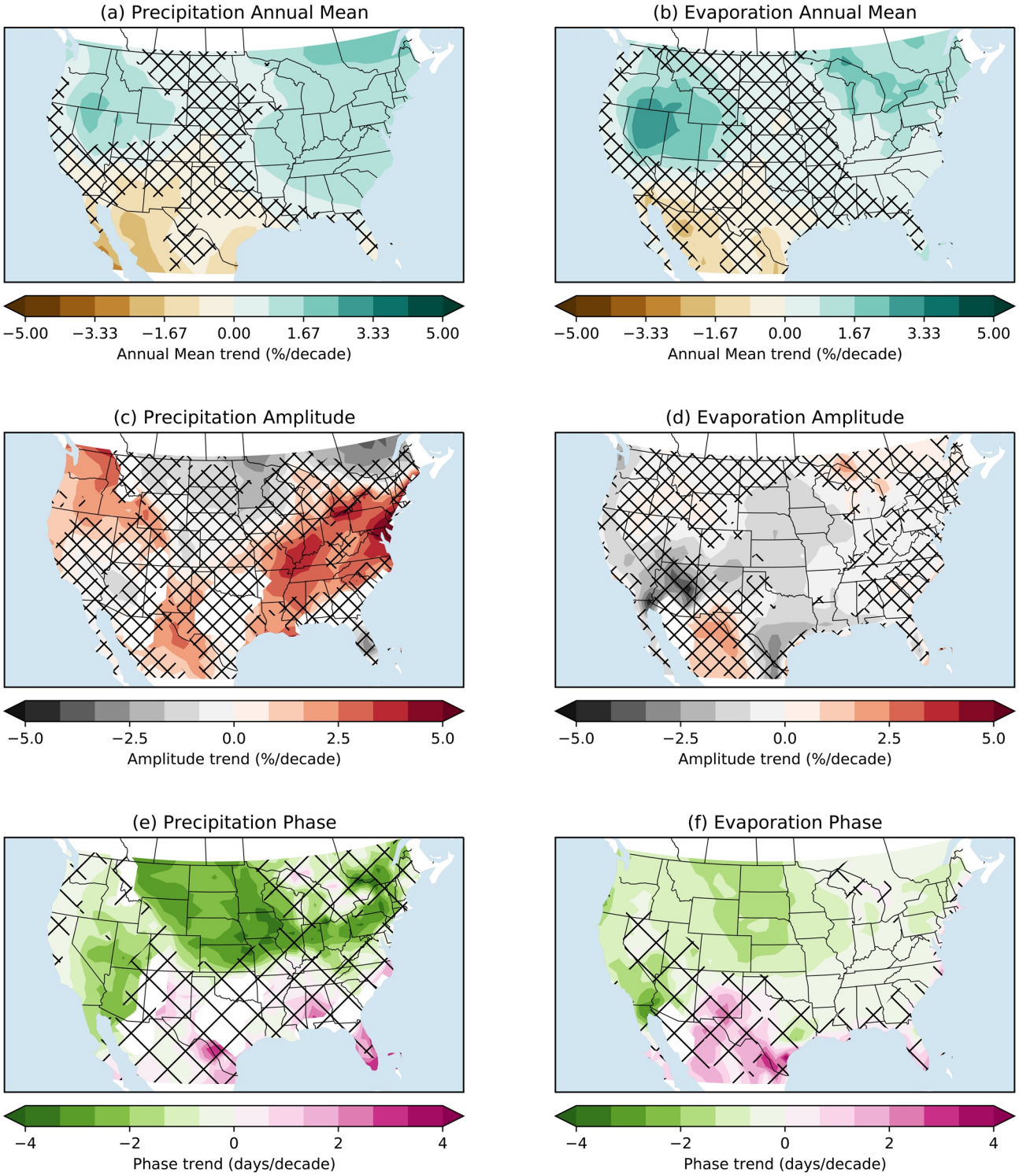

Figure 6. Multi-model mean projected 2015–2100 trends under SSP5-8.5 in the annual mean (a and b), amplitude (c and d), and phase (e and f) of the annual cycle for precipitation and evaporation. Hatching indicates regions where fewer than 75% of models agree on the sign of the trends.

saturated. This inundation prevents a decrease in the total column soil moisture in the Southeast, but much of it is not stored in the soil column and instead shed as runoff. Meanwhile, increasing temperatures and evaporative demand dry the surface soil moisture despite the seasonal increase in rainfall. The central portions of the country are the only regions projected to experience little change in total

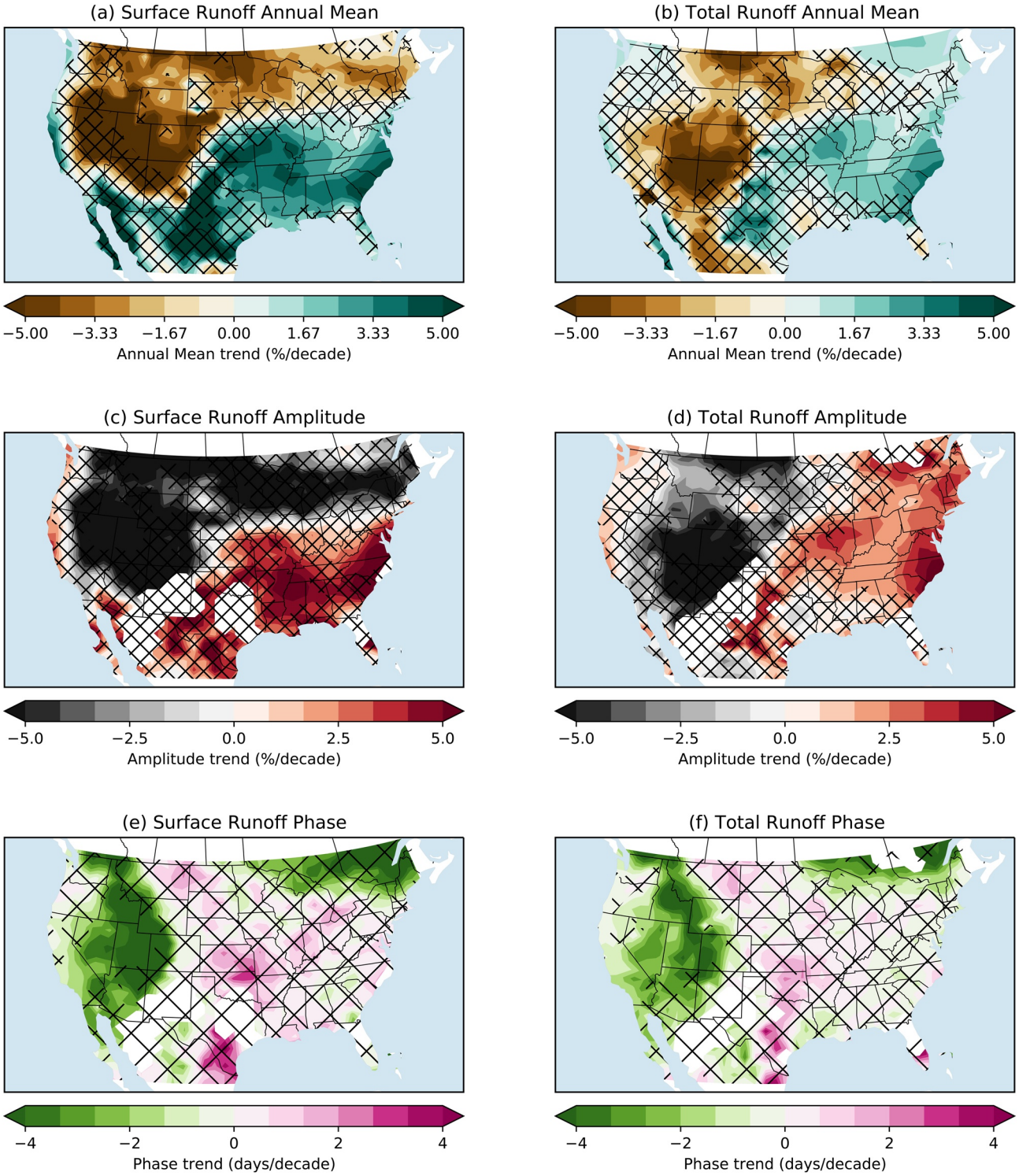

Figure 7. Multi-model mean projected 2015–2100 trends under SSP5-8.5 in the annual mean (a and b), amplitude (c and d), and phase (e and f) of the annual cycle for surface and total runoff. Hatching indicates regions where fewer than 75% of models agree on the sign of the trends.

soil moisture during the wet season, but a large decrease in total soil moisture in the dry season. This is largely attributable to seasonal shifts in precipitation. In the upper Great Plains and Midwest, the bulk of rainfall occurs during the April-September growing season (Helfand & Schubert, 1995; Walters & Winkler, 2001). CMIP6 models project earlier onset and an earlier peak in this rainfall, which translates to

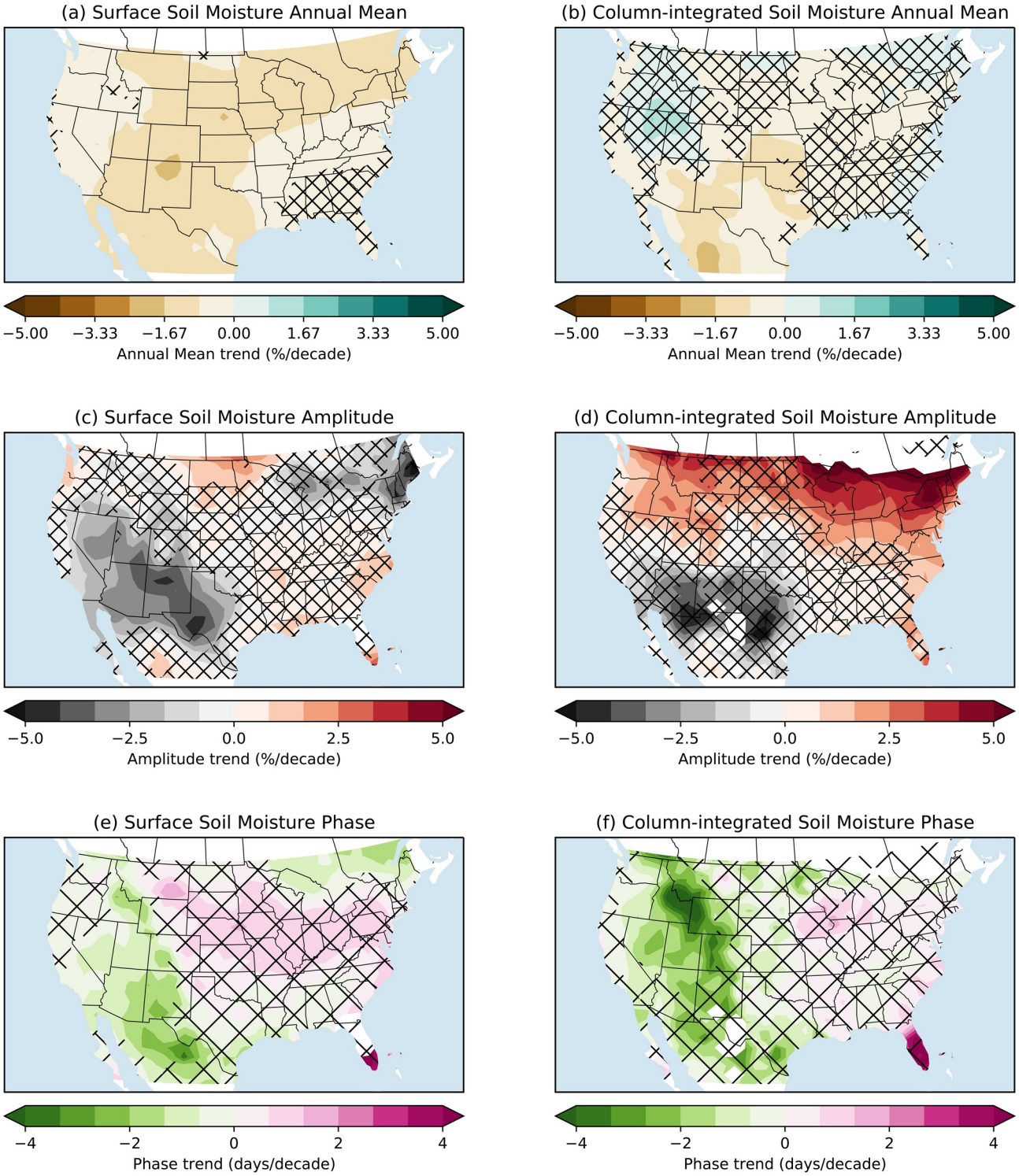

Figure 8. Multi-model mean projected 2015–2100 trends under SSP5-8.5 in the annual mean (a and b), amplitude (c and d), and phase (e and f) of the annual cycle for surface and column-integrated runoff. Hatching indicates regions where fewer than 75% of models agree on the sign of the trends.

an earlier peak in total soil moisture. Because the bulk of the supply of moisture, in the form of rainfall, arrives significantly earlier, these regions are projected to experience summer drying throughout the soil moisture column.

5. Conclusions

Our results reveal many coherent changes across sixteen state-of-the-art climate models (Eyring et al., 2016) and four future emissions scenarios (O'Neill et al., 2016). They indicate that analyses focusing on annual (e.g., Bonfils et al., 2020; Zhang et al., 2007) or seasonal (e.g., Cook et al., 2020) mean changes, while useful, may miss important shifts in the amplitude or phase of the annual cycle. These shifts may have real-world consequences for water management, agriculture, and other crucial sectors (Seneviratne et al., 2012), and can help to illustrate the physical drivers that affect drought risk in different regions. The CMIP6 models project slight increases or no significant change to annual mean precipitation throughout the CONUS regions, no significant changes to the precipitation annual cycle amplitude, and substantial phase delays to the precipitation annual cycle in only two regions (the upper Great Plains and Midwest). However, CMIP6 models project all significant shifts in the annual mean and the annual cycle of evaporation, surface and total runoff, and surface and total soil moisture, even in the absence of precipitation shifts. Further understanding the mechanisms that create these shifts to earlier peaks, and confirming that the models are indeed accurately simulating these annual cycle changes, is important for future work.

All future projections are highly sensitive to the future scenario used: in no region, and for no variable, is there a detectable (at the 90% confidence level) change to the amplitude or phase or the annual cycle in the low-forcing SSP1-2.6 scenario. Very few variables other than temperature show annual mean changes that exceed this threshold in this scenario. This indicates that the large-scale shifts in the timing and amount of these variables projected in the highest-forcing, worst-case scenarios are largely avoidable with aggressive mitigation efforts.

In the absence of such mitigation efforts, the United States will need to adapt to multiple significant and interlinked changes in hydroclimate. Climate models project not only robust changes in multiple climate variables, but significant changes to their annual cycles. Adaptation decisions therefore must consider such seasonal shifts, and strategies predicated on existing annual cycles may not be optimal in the future. For example, reservoir management strategies organized around managing wintertime flooding and relying on spring snowmelt to recharge water supply for the summer may not be appropriate in a climate-changed world. Existing planting and harvesting strategies would similarly need to confront potentially different growing seasons in the future. The state-of-the-art climate models participating in CMIP6 indicate that flexible adaptation strategies, able to cope with shifts in the amount, distribution, and timing of multiple climate variables, will be necessary to confront a world in which greenhouse gas emissions continue to increase.

Acknowledgments
B. I. Cook, K. Marvel, and A. P. Williams were all supported by the NOAA MAPP grant, "Integrating models, paleoclimate, and recent observations to develop process-level understanding of projected changes in U.S. drought." This work benefited from participation by B. I. Cook and A. P. Williams in the NOAA CMIP6 Task Force, which is co-led by K. Marvel. The authors thank Naomi Henderson at the Lamont-Doherty Earth Observatory for essential help organizing output from the CMIP6 models and Gianna Lum for help determining the regional boundaries. C. J. W. Bonfils's work was performed under the auspices of the US Department of Energy (DOE) by Lawrence Livermore National Laboratory under contract no. DE-AC52-07NA27344; she was supported by the DOE Regional and Global Model Analysis Program under the PCMDI SFA, and the grant no. DE-SC0014423. J. E. Smerdon was supported in part by the National Science Foundation grant AGS-1805490 and the National Oceanic and Atmospheric Administration grant NA20OAR4310425.

Data Availability Statement

All data from CMIP6 simulations used in our analyses are freely available from the Earth System Grid Federation (https://esgf-node.llnl.gov/search/cmip6/).

References

Allen, M. R., & Ingram, W. J. (2002). Constraints on future changes in climate and the hydrologic cycle. *Nature*, *419*(6903), 224–232. https://doi.org/10.1038/nature01092

Barnett, T. P., Adam, J. C., & Lettenmaier, D. P. (2005). Potential impacts of a warming climate on water availability in snow-dominated regions. *Nature*, *438*(7066), 303–309. https://doi.org/10.1038/nature04141

Barnett, T. P., Pierce, D. W., Hidalgo, H. G., Bonfils, C., Santer, B. D., Das, T., et al. (2008). Human-induced changes in the hydrology of the western United States. *Science*, *319*(5866), 1080–1083. https://doi.org/10.1126/science.1152538

Berg, A., Sheffield, J., & Milly, P. C. D. (2017). Divergent surface and total soil moisture projections under global warming. *Geophysical Research Letters*, *44*(1), 236–244. https://doi.org/10.1002/2016gl071921

Bindoff, N., Stott, P., AchutaRao, K., Allen, M., Gillett, N., Gutzler, D., et al. (2013). Detection and attribution of climate change: From global to regional [Book Section]. In T. F. Stocker, D. Qin, G.-K. Plattner, M. Tignor, S. K. Allen, J. Boschung, et al. (Eds.), *Climate change 2013: The physical science basis. Contribution of working group I to the fifth assessment report of the Intergovernmental Panel on Climate Change* (pp. 867–952). Cambridge University Press. Retrieved from www.climatechange2013.org

Bonfils, C. J., Anderson, G., Santer, B. D., Phillips, T. J., Taylor, K. E., Cuntz, M., et al. (2017). Competing influences of anthropogenic warming, ENSO, and plant physiology on future terrestrial aridity. *Journal of Climate*, *30*(17), 6883–6904. https://doi.org/10.1175/jcli-d-17-0005.1

Bonfils, C. J., Santer, B. D., Fyfe, J. C., Marvel, K., Phillips, T. J., & Zimmerman, S. R. (2020). Human influence on joint changes in temperature, rainfall and continental aridity. *Nature Climate Change*, *10*(8), 726–731. https://doi.org/10.1038/s41558-020-0821-1

Boucher, O., Denvil, S., Caubel, A., & Foujols, M. A. (2018). *IPSL IPSL-CM6A-LR model output prepared for CMIP6 CMIP*. Earth System Grid Federation. Retrieved from http://cera-www.dkrz.de/WDCC/meta/CMIP6/CMIP6.CMIP.IPSL.IPSL-CM6A-LR

Byrne, M. P., & O'Gorman, P. A. (2015). The response of precipitation minus evapotranspiration to climate warming: Why the wet-get-wetter, dry-get-drier scaling does not hold over land. *Journal of Climate*, *28*(20), 8078–8092. https://doi.org/10.1175/jcli-d-15-0369.1

Chou, C., & Lan, C.-W. (2012). Changes in the annual range of precipitation under global warming. *Journal of Climate*, *25*(1), 222–235. https://doi.org/10.1175/jcli-d-11-00097.1

Cook, B. I., Ault, T. R., & Smerdon, J. E. (2015). Unprecedented 21st century drought risk in the American Southwest and Central Plains. *Science Advances*, *1*(1), e1400082. https://doi.org/10.1126/sciadv.1400082

Cook, B. I., Mankin, J. S., & Anchukaitis, K. J. (2018). Climate change and drought: From past to future. *Current Climate Change Reports*, *4*(2), 164–179. https://doi.org/10.1007/s40641-018-0093-2

Cook, B. I., Mankin, J. S., Marvel, K., Williams, A. P., Smerdon, J. E., & Anchukaitis, K. J. (2020). Twenty-first century drought projections in the CMIP6 forcing scenarios. *Earth's Future*, *8*(6), e2019EF001461. https://doi.org/10.1029/2019ef001461

Cook, B. I., Mankin, J. S., Williams, A. P., Marvel, K., Smerdon, J. E., & Liu, H. (2021). Uncertainties, limits, and benefits of climate change mitigation for soil moisture drought in Southwestern North America. *Earth's Future*. https://doi.org/10.1029/2021EF002014

Danabasoglu, G. (2019). *NCAR CESM2 model output prepared for CMIP6 ScenarioMIP*. Earth System Grid Federation. Retrieved from http://cera-www.dkrz.de/WDCC/meta/CMIP6/CMIP6.ScenarioMIP.NCAR.CESM2

Dettinger, M. D., & Cayan, D. R. (1995). Large-scale atmospheric forcing of recent trends toward early snowmelt runoff in California. *Journal of Climate*, *8*(3), 606–623. https://doi.org/10.1175/1520-0442(1995)008<0606:lsafor>2.0.co;2

Diffenbaugh, N. S., Scherer, M., & Trapp, R. J. (2013). Robust increases in severe thunderstorm environments in response to greenhouse forcing. *Proceedings of the National Academy of Sciences*, *110*(41), 16361–16366. https://doi.org/10.1073/pnas.1307758110

Dix, M., Bi, D., Dobrohotoff, P., Fiedler, R., Harman, I., Law, R., et al. (2019). *CSIRO-ARCCSS ACCESS-CM2 model output prepared for CMIP6 CMIP historical*. Earth System Grid Federation. Retrieved from http://cera-www.dkrz.de/WDCC/meta/CMIP6/CMIP6.CMIP.CSIRO-ARCCSS.ACCESS-CM2.historical

Dwyer, J. G., Biasutti, M., & Sobel, A. H. (2012). Projected changes in the seasonal cycle of surface temperature. *Journal of Climate*, *25*(18), 6359–6374. https://doi.org/10.1175/jcli-d-11-00741.1

Dwyer, J. G., Biasutti, M., & Sobel, A. H. (2014). The effect of greenhouse gas–induced changes in SST on the annual cycle of zonal mean tropical precipitation. *Journal of Climate*, *27*(12), 4544–4565. https://doi.org/10.1175/jcli-d-13-00216.1

EC-Earth Consortium (EC-Earth). (2019a). *EC-Earth-consortium EC-Earth3 model output prepared for CMIP6 ScenarioMIP*. Earth System Grid Federation. Retrieved from http://cera-www.dkrz.de/WDCC/meta/CMIP6/CMIP6.ScenarioMIP.EC-Earth-Consortium.EC-Earth3

EC-Earth Consortium (EC-Earth). (2019b). *EC-Earth-Consortium EC-Earth3-Veg model output prepared for CMIP6 ScenarioMIP*. Earth System Grid Federation. Retrieved from http://cera-www.dkrz.de/WDCC/meta/CMIP6/CMIP6.ScenarioMIP.EC-Earth-Consortium.EC-Earth3-Veg

Eyring, V., Bony, S., Meehl, G. A., Senior, C. A., Stevens, B., Stouffer, R. J., & Taylor, K. E. (2016). Overview of the Coupled Model Intercomparison Project Phase 6 (CMIP6) experimental design and organization. *Geoscientific Model Development*, *9*(5), 1937–1958. https://doi.org/10.5194/gmd-9-1937-2016

Good, P., Sellar, A., Tang, Y., Rumbold, S., Ellis, R., Kelley, D., et al. (2019). *MOHC UKESM1.0-LL model output prepared for CMIP6 ScenarioMIP*. Earth System Grid Federation. Retrieved from http://cera-www.dkrz.de/WDCC/meta/CMIP6/CMIP6.ScenarioMIP.MOHC.UKESM1-0-LL

Guo, H., John, J. G., Blanton, C., McHugh, C., Nikonov, S., Radhakrishnan, A., et al. (2018). *NOAA-GFDL GFDL-CM4 model output*. Earth System Grid Federation. Retrieved from http://cera-www.dkrz.de/WDCC/meta/CMIP6/CMIP6.CMIP.NOAA-GFDL.GFDL-CM4

Hamlet, A. F., Mote, P. W., Clark, M. P., & Lettenmaier, D. P. (2005). Effects of temperature and precipitation variability on snowpack trends in the western United States. *Journal of Climate*, *18*(21), 4545–4561. https://doi.org/10.1175/jcli3538.1

Hegerl, G. C., Black, E., Allan, R. P., Ingram, W. J., Polson, D., Trenberth, K. E., et al. (2015). Challenges in quantifying changes in the global water cycle. *Bulletin of the American Meteorological Society*, *96*(7), 1097–1115. https://doi.org/10.1175/bams-d-13-00212.1

Held, I. M., & Soden, B. J. (2006). Robust responses of the hydrological cycle to global warming. *Journal of Climate*, *19*(21), 5686–5699. https://doi.org/10.1175/jcli3990.1

Helfand, H. M., & Schubert, S. D. (1995). Climatology of the simulated Great Plains low-level jet and its contribution to the continental moisture budget of the United States. *Journal of Climate*, *8*(4), 784–806. https://doi.org/10.1175/1520-0442(1995)008<0784:cotsgp>2.0.co;2

Hurk, B. V. D., Kim, H., Krinner, G., Seneviratne, S. I., Derksen, C., Oki, T., et al. (2016). LS3MIP (v1. 0) contribution to CMIP6: The land surface, snow and soil moisture model intercomparison project–aims, setup and expected outcome. *Geoscientific Model Development*, *9*(8), 2809–2832. https://doi.org/10.5194/gmd-9-2809-2016

Kelley, C. P., Mohtadi, S., Cane, M. A., Seager, R., & Kushnir, Y. (2015). Climate change in the Fertile Crescent and implications of the recent Syrian drought. *Proceedings of the National Academy of Sciences*, *112*(11), 3241–3246. https://doi.org/10.1073/pnas.1421533112

Knowles, N., Dettinger, M. D., & Cayan, D. R. (2006). Trends in snowfall versus rainfall in the western United States. *Journal of Climate*, *19*(18), 4545–4559. https://doi.org/10.1175/jcli3850.1

Lehner, F., Wood, A. W., Vano, J. A., Lawrence, D. M., Clark, M. P., & Mankin, J. S. (2019). The potential to reduce uncertainty in regional runoff projections from climate models. *Nature Climate Change*, *9*(12), 926–933. https://doi.org/10.1038/s41558-019-0639-x

Levy, A. A., Ingram, W., Jenkinson, M., Huntingford, C., Hugo Lambert, F., & Allen, M. (2013). Can correcting feature location in simulated mean climate improve agreement on projected changes? *Geophysical Research Letters*, *40*(2), 354–358. https://doi.org/10.1002/2012gl053964

Mankin, J. S., Seager, R., Smerdon, J. E., Cook, B. I., & Williams, A. P. (2019). Mid-latitude freshwater availability reduced by projected vegetation responses to climate change. *Nature Geoscience*, *12*(12), 983–988. https://doi.org/10.1038/s41561-019-0480-x

Mankin, J. S., Smerdon, J. E., Cook, B. I., Williams, A. P., & Seager, R. (2017). The curious case of projected twenty-first-century drying but greening in the American West. *Journal of Climate*, *30*(21), 8689–8710. https://doi.org/10.1175/jcli-d-17-0213.1

Mann, M. E., & Park, J. (1996). Greenhouse warming and changes in the seasonal cycle of temperature: Model versus observations. *Geophysical Research Letters*, *23*(10), 1111–1114. https://doi.org/10.1029/96gl01066

Marvel, K., Biasutti, M., Bonfils, C., Taylor, K. E., Kushnir, Y., & Cook, B. I. (2017). Observed and projected changes to the precipitation annual cycle. *Journal of Climate*, *30*(13), 4983–4995. https://doi.org/10.1175/jcli-d-16-0572.1

Marvel, K., & Bonfils, C. (2013). Identifying external influences on global precipitation. *Proceedings of the National Academy of Sciences*, *110*(48), 19301–19306. https://doi.org/10.1073/pnas.1314382110

Marvel, K., Cook, B. I., Bonfils, C. J., Durack, P. J., Smerdon, J. E., & Williams, A. P. (2019). Twentieth-century hydroclimate changes consistent with human influence. *Nature*, *569*(7754), 59–65. https://doi.org/10.1038/s41586-019-1149-8

Marvel, K., Ivanova, D., & Taylor, K. (2013). Scale space methods for climate model analysis. *Journal of Geophysical Research: Atmospheres*, *118*(11), 5082–5097. https://doi.org/10.1002/jgrd.50433

Masson, D., & Knutti, R. (2011). Climate model genealogy. *Geophysical Research Letters*, *38*(8). https://doi.org/10.1029/2011gl046864

Meehl, G. A., Senior, C. A., Eyring, V., Flato, G., Lamarque, J.-F., Stouffer, R. J., et al. (2020). Context for interpreting equilibrium climate sensitivity and transient climate response from the CMIP6 Earth system models. *Science Advances*, *6*(26), eaba1981. https://doi.org/10.1126/sciadv.aba1981

Milly, P. C., & Dunne, K. A. (2016). Potential evapotranspiration and continental drying. *Nature Climate Change*, *6*(10), 946–949. https://doi.org/10.1038/nclimate3046

Milly, P. C., Dunne, K. A., & Vecchia, A. V. (2005). Global pattern of trends in streamflow and water availability in a changing climate. *Nature*, *438*(7066), 347–350. https://doi.org/10.1038/nature04312

Mueller, B., & Seneviratne, S. I. (2014). Systematic land climate and evapotranspiration biases in CMIP5 simulations. *Geophysical Research Letters*, *41*(1), 128–134. https://doi.org/10.1002/2013gl058055

Neelin, J., Chou, C., & Su, H. (2003). Tropical drought regions in global warming and El Nino teleconnections. *Geophysical Research Letters*, *30*(24). https://doi.org/10.1029/2003gl018625

O'Gorman, P. A., & Schneider, T. (2009). The physical basis for increases in precipitation extremes in simulations of 21st-century climate change. *Proceedings of the National Academy of Sciences*, *106*(35), 14773–14777.

O'Neill, B. C., Tebaldi, C., Van Vuuren, D. P., Eyring, V., Friedlingstein, P., Hurtt, G., et al. (2016). The scenario model intercomparison project (ScenarioMIP) for CMIP6. *Geoscientific Model Development*, *9*(9), 3461–3482. https://doi.org/10.5194/gmd-9-3461-2016

Parmesan, C., & Yohe, G. (2003). A globally coherent fingerprint of climate change impacts across natural systems. *Nature*, *421*(6918), 37–42. https://doi.org/10.1038/nature01286

Pendergrass, A. G., & Hartmann, D. L. (2014). The atmospheric energy constraint on global-mean precipitation change. *Journal of Climate*, *27*(2), 757–768. https://doi.org/10.1175/jcli-d-13-00163.1

Reidmiller, D. R., Avery, C. W., Easterling, D. R., Kunkel, K. E., Lewis, K. L., Maycock, T., & Stewart, B. C. (2017). *Impacts, risks, and adaptation in the United States: Fourth national climate assessment, volume II*.

Sanderson, B. M., Wehner, M., & Knutti, R. (2017). Skill and independence weighting for multi-model assessments. *Geoscientific Model Development*, *10*(6), 2379–2395. https://doi.org/10.5194/gmd-10-2379-2017

Santer, B. D., Mears, C., Doutriaux, C., Caldwell, P., Gleckler, P., Wigley, T., et al. (2011). Separating signal and noise in atmospheric temperature changes: The importance of timescale. *Journal of Geophysical Research: Atmospheres*, *116*(D22). https://doi.org/10.1029/2011jd016263

Santer, B. D., Mears, C., Wentz, F., Taylor, K., Gleckler, P., Wigley, T., et al. (2007). Identification of human-induced changes in atmospheric moisture content. *Proceedings of the National Academy of Sciences*, *104*(39), 15248–15253. https://doi.org/10.1073/pnas.0702872104

Santer, B. D., Mikolajewicz, U., Brüggemann, W., Cubasch, U., Hasselmann, K., Höck, H., et al. (1995). Ocean variability and its influence on the detectability of greenhouse warming signals. *Journal of Geophysical Research*, *100*(C6), 10693–10710. https://doi.org/10.1029/95jc00683

Santer, B. D., Painter, J. F., Mears, C. A., Doutriaux, C., Caldwell, P., Arblaster, J. M., et al. (2013). Identifying human influences on atmospheric temperature. *Proceedings of the National Academy of Sciences*, *110*(1), 26–33. https://doi.org/10.1073/pnas.1210514109

Santer, B. D., Po-Chedley, S., Zelinka, M. D., Cvijanovic, I., Bonfils, C., Durack, P. J., et al. (2018). Human influence on the seasonal cycle of tropospheric temperature. *Science*, *361*(6399). https://doi.org/10.1126/science.aas8806

Sarojini, B. B., Stott, P. A., & Black, E. (2016). Detection and attribution of human influence on regional precipitation. *Nature Climate Change*, *6*(7), 669–675. https://doi.org/10.1038/nclimate2976

Scheff, J., & Frierson, D. M. (2012). Robust future precipitation declines in CMIP5 largely reflect the poleward expansion of model subtropical dry zones. *Geophysical Research Letters*, *39*(18). https://doi.org/10.1029/2012gl052910

Schneider, T., Bischoff, T., & Haug, G. H. (2014). Migrations and dynamics of the intertropical convergence zone. *Nature*, *513*(7516), 45–53. https://doi.org/10.1038/nature13636

Schumacher, R. S., & Rasmussen, K. L. (2020). The formation, character and changing nature of mesoscale convective systems. *Nature Reviews Earth & Environment*, *1*(6), 300–314. https://doi.org/10.1038/s43017-020-0057-7

Schupfner, M., Wieners, K.-H., Wachsmann, F., Steger, C., Bittner, M., Jungclaus, J., et al. (2019). *DKRZ MPI-ESM1.2-HR model output prepared for CMIP6 ScenarioMIP*. Earth System Grid Federation. Retrieved from http://cera-www.dkrz.de/WDCC/meta/CMIP6/CMIP6.ScenarioMIP.DKRZ.MPI-ESM1-2-HR

Scranton, K., & Amarasekare, P. (2017). Predicting phenological shifts in a changing climate. *Proceedings of the National Academy of Sciences*, *114*(50), 13212–13217. https://doi.org/10.1073/pnas.1711221114

Seeley, J. T., & Romps, D. M. (2015). The effect of global warming on severe thunderstorms in the United States. *Journal of Climate*, *28*(6), 2443–2458. https://doi.org/10.1175/jcli-d-14-00382.1

Seferian, R. (2019). *CNRM-CERFACS CNRM-ESM2-1 model output prepared for CMIP6 ScenarioMIP*. Earth System Grid Federation. Retrieved from http://cera-www.dkrz.de/WDCC/meta/CMIP6/CMIP6.ScenarioMIP.CNRM-CERFACS.CNRM-ESM2-1

Seneviratne, S., Nicholls, N., Easterling, D., Goodess, C., Kanae, S., Kossin, J., et al. (2012). *Managing the risks of extreme events and disasters to advance climate change adaptation a special report of Working Groups I and II of the Intergovernmental Panel on Climate Change (IPCC)*. Cambridge University Press.

Seth, A., Rauscher, S. A., Biasutti, M., Giannini, A., Camargo, S. J., & Rojas, M. (2013). CMIP5 projected changes in the annual cycle of precipitation in monsoon regions. *Journal of Climate*, *26*(19), 7328–7351. https://doi.org/10.1175/jcli-d-12-00726.1

Shiogama, H., Abe, M., & Tatebe, H. (2019). *MIROC MIROC6 model output prepared for CMIP6 ScenarioMIP*. Earth System Grid Federation. Retrieved from http://cera-www.dkrz.de/WDCC/meta/CMIP6/CMIP6.ScenarioMIP.MIROC.MIROC6

Sillmann, J., Kharin, V., Zhang, X., Zwiers, F., & Bronaugh, D. (2013). Climate extremes indices in the CMIP5 multimodel ensemble: Part 1. Model evaluation in the present climate. *Journal of Geophysical Research: Atmospheres*, *118*(4), 1716–1733. https://doi.org/10.1002/jgrd.50203

Stine, A., Huybers, P., & Fung, I. (2009). Changes in the phase of the annual cycle of surface temperature. *Nature*, *457*(7228), 435–440. https://doi.org/10.1038/nature07675

Stott, P. A., Gillett, N. P., Hegerl, G. C., Karoly, D. J., Stone, D. A., Zhang, X., & Zwiers, F. (2010). Detection and attribution of climate change: A regional perspective. *Wiley Interdisciplinary Reviews: Climate Change*, *1*(2), 192–211. https://doi.org/10.1002/wcc.34

Swann, A. L., Hoffman, F. M., Koven, C. D., & Randerson, J. T. (2016). Plant responses to increasing CO_2 reduce estimates of climate impacts on drought severity. *Proceedings of the National Academy of Sciences*, *113*(36), 10019–10024. https://doi.org/10.1073/pnas.1604581113

Swart, N. C., Cole, J. N., Kharin, V. V., Lazare, M., Scinocca, J. F., Gillett, N. P., et al. (2019). *CCCma CanESM5 model output prepared for CMIP6 ScenarioMIP*. Earth System Grid Federation. Retrieved from http://cera-www.dkrz.de/WDCC/meta/CMIP6/CMIP6.ScenarioMIP.CCCma.CanESM5

Tachiiri, K., Abe, M., Hajima, T., Arakawa, O., Suzuki, T., Komuro, Y., et al. (2019). *MIROC MIROC-ES2L model output prepared for CMIP6 ScenarioMIP*. Earth System Grid Federation. Retrieved from http://cera-www.dkrz.de/WDCC/meta/CMIP6/CMIP6.ScenarioMIP.MIROC.MIROC-ES2L

Tang, Y., Winkler, J., Zhong, S., Bian, X., Doubler, D., Yu, L., & Walters, C. (2017). Future changes in the climatology of the Great Plains low-level jet derived from fine resolution multi-model simulations. *Scientific Reports*, *7*(1), 1–10. https://doi.org/10.1038/s41598-017-05135-0

Tian, B., & Dong, X. (2020). The double-ITCZ bias in CMIP3, CMIP5, and CMIP6 models based on annual mean precipitation. *Geophysical Research Letters*, *47*(8), e2020GL087232. https://doi.org/10.1029/2020gl087232

Voldoire, A. (2019). *CNRM-CERFACS CNRM-CM6-1 model output prepared for CMIP6 ScenarioMIP*. Earth System Grid Federation. Retrieved from http://cera-www.dkrz.de/WDCC/meta/CMIP6/CMIP6.ScenarioMIP.CNRM-CERFACS.CNRM-CM6-1

Walters, C. K., & Winkler, J. A. (2001). Airflow configurations of warm season southerly low-level wind maxima in the Great Plains. Part I: Spatial and temporal characteristics and relationship to convection. *Weather and Forecasting*, *16*(5), 513–530. https://doi.org/10.1175/1520-0434(2001)016<0513:acowss>2.0.co;2

Weigel, A. P., Knutti, R., Liniger, M. A., & Appenzeller, C. (2010). Risks of model weighting in multimodel climate projections. *Journal of Climate*, *23*(15), 4175–4191. https://doi.org/10.1175/2010jcli3594.1

Wentz, F. J., Ricciardulli, L., Hilburn, K., & Mears, C. (2007). How much more rain will global warming bring? *Science*, *317*(5835), 233–235. https://doi.org/10.1126/science.1140746

Westerling, A. L. (2016). Increasing western US forest wildfire activity: Sensitivity to changes in the timing of spring. *Philosophical Transactions of the Royal Society B: Biological Sciences*, *371*(1696), 20150178. https://doi.org/10.1098/rstb.2015.0178

Williams, A. P., Cook, E. R., Smerdon, J. E., Cook, B. I., Abatzoglou, J. T., Bolles, K., et al. (2020). Large contribution from anthropogenic warming to an emerging North American megadrought. *Science*, *368*(6488), 314–318. https://doi.org/10.1126/science.aaz9600

Wood, A. W., Lettenmaier, D. P., & Palmer, R. N. (1997). Assessing climate change implications for water resources planning. In *Climate change and water resources planning criteria* (pp. 203–228). Springer. https://doi.org/10.1007/978-94-017-1051-0_12

Xin, X., Wu, T., Shi, X., Zhang, F., Li, J., Chu, M., et al. (2019). *BCC BCC-CSM2MR model output prepared for CMIP6 ScenarioMIP*. Earth System Grid Federation. Retrieved from http://cera-www.dkrz.de/WDCC/meta/CMIP6/CMIP6.ScenarioMIP.BCC.BCC-CSM2-MR

Yukimoto, S., Koshiro, T., Kawai, H., Oshima, N., Yoshida, K., Urakawa, S., et al. (2019). *MRI MRI-ESM2.0 model output prepared for CMIP6 ScenarioMIP*. Earth System Grid Federation. Retrieved from http://cera-www.dkrz.de/WDCC/meta/CMIP6/CMIP6.ScenarioMIP.MRI.MRI-ESM2-0

Zelinka, M. D., Myers, T. A., McCoy, D. T., Po-Chedley, S., Caldwell, P. M., Ceppi, P., et al. (2020). Causes of higher climate sensitivity in CMIP6 models. *Geophysical Research Letters*, *47*(1), e2019GL085782. https://doi.org/10.1029/2019gl085782

Zhang, X., Zwiers, F. W., Hegerl, G. C., Lambert, F. H., Gillett, N. P., Solomon, S., et al. (2007). Detection of human influence on twentieth-century precipitation trends. *Nature*, *448*(7152), 461–465. https://doi.org/10.1038/nature06025

Ziehn, T., Chamberlain, M., Lenton, A., Law, R., Bodman, R., Dix, M., et al. (2019). *CSIRO ACCESS-ESM1.5 model output prepared for CMIP6 ScenarioMIP*. Earth System Grid Federation. Retrieved from http://cera-www.dkrz.de/WDCC/meta/CMIP6/CMIP6.ScenarioMIP.CSIRO.ACCESS-ESM1-5